Ramsey Spectroscopy of the math xmlns="http://www.w3.org/1998/Math/MathML" display="inline">mrow>mn>2/mn>msub>mrow>mi mathvariant="normal">S/mi>/mrow>mrow>mn>1/mn>mo>//mo>mn>2/mn>/mrow>/msub>/mrow>/math> Hyperfine Interval in Atomic Hydrogen

R. G. Bullis, C. Rasor, W. L. Tavis, S. A. Johnson, M. R. Weiss, and D. C. Yost

Phys. Rev. Lett. **130**, 203001 — Published 18 May 2023

DOI: 10.1103/PhysRevLett.130.203001

Ramsey spectroscopy of the $2S_{1/2}$ hyperfine interval in atomic hydrogen

R. G. Bullis, C. Rasor, W. L. Tavis, S. A. Johnson, M. R. Weiss, and D. C. Yost
Department of Physics, Colorado State University, Fort Collins, Colorado, 80523, USA

The $2S_{1/2}$ hyperfine interval in atomic hydrogen was measured using Ramsey spectroscopy with a thermal beam cooled to cryogenic temperatures. The measured value is 177 556 838.87(85) Hz, which represents the most precise determination of this interval to date. The $1S_{1/2}$ hyperfine interval, $f(1S_{1/2})$, and the $2S_{1/2}$ hyperfine interval, $f(2S_{1/2})$, can be combined to give the quantity $D_{21} = 8\,f(2S_{1/2}) - f(1S_{1/2})$, which mostly eliminates uncertainty due to nuclear structure effects and is well-described by bound-state quantum electrodynamics. Using the value of $f(2S_{1/2})$ from this work gives a value of $D_{21}^{\rm Exp} = 48\,959.2(6.8)$ Hz, which is in agreement with the theoretical value of $D_{21}^{\rm Theory} = 48\,954.1(2.3)$ Hz.

The simple structure of the hydrogen atom allows for precise calculations that can be compared with experiment. Not only has hydrogen been used to determine fundamental constants, such as the proton charge radius and the Rydberg constant [1], but it has also been used as a theoretical testing ground for quantum mechanics and quantum electrodynamics (QED) for over a century. Using hydrogen masers, the ground state hyperfine interval in atomic hydrogen has been measured extremely precisely, with a relative uncertainty of roughly 10^{-12} [2–5]. Calculations of this transition with QED corrections are available [6–8]. Unfortunately, a comparison of the experimentally determined value with theory is limited by an insufficient understanding of proton structure effects [11]. However, a linear combination of the $1S_{1/2}$ and $2S_{1/2}$ hyperfine intervals given by

$$D_{21} = 8\,f(2S_{1/2}) - f(1S_{1/2}), \qquad (1)$$

largely eliminates the theoretical uncertainty in nuclear structure and is a stringent test of fourth-order bound-state QED [6–8, 12–16]. In 2002, the theoretical value of D_{21} was calculated including fourth-order QED corrections [6, 7]. The value was updated slightly in 2006 after re-evaluating the self-energy correction and adding a numerically small logarithmic recoil correction [8]. A high-precision numerical calculation of the self-energy was then performed in 2008, resulting in $D_{21}^{\rm Theory} = 48\,954.1(2.3)$ Hz [9], which is the most up-to-date published value.

In addition to bound-state QED tests, several authors have noted that measurements of D_{21} can be used to provide constraints on light bosons with weak coupling to Standard Model particles [17–19]. Such hypothetical particles could manifest themselves by producing an additional spin-dependent interaction between the proton and electron, which would cause a deviation between the experimental and theoretical values of D_{21}.

Due to the very high precision of the ground state hyperfine measurements, the experimentally determined values of D_{21} in atomic hydrogen are limited by the uncertainty in measurements of the $2S_{1/2}$ hyperfine interval. While direct measurements of this magnetic-dipole radio-frequency (RF) transition have been performed in the past [20, 21], substantial improvements in precision optical spectroscopy have also allowed for measurements through the $1S_{1/2}$–$2S_{1/2}$ two-photon optical transition [22, 23]. The most recent optical measurement was $f(2S_{1/2}) = 177\,556\,834.3(6.7)$ Hz, resulting in $D_{21}^{\rm Exp} = 48\,923(54)$ Hz, which is in good agreement with theory.

Here, we present an RF measurement of the $2S_{1/2}$ hyperfine interval using Ramsey's method of separated oscillatory fields. The last measurement using Ramsey's method was performed by Heberle, Reich, and Kusch in 1956 [20]. In addition to the general advances in experimental equipment and techniques since that time, we notably have the ability to selectively populate the $2S_{1/2}^{F=0}$ state using the $1S_{1/2}$ - $2S_{1/2}$ two-photon transition before spectroscopy (as in [24, 25]). This simplifies the RF measurement and allows for the adjustment of the mean velocity of our atomic beam through the control of our cryogenic nozzle. These advances have allowed for a reduction in the uncertainty of $D_{21}^{\rm Exp}$ by a factor of ≈ 8 as compared to the previous best optical measurement [23], and by a factor of ≈ 60 as compared to the previous measurement using RF Ramsey spectroscopy [20].

The experimental apparatus to generate cryogenic $2S_{1/2}^{F=0}$ or $2S_{1/2}^{F=1}$ hydrogen atoms has been previously described in [25]. Additionally, the velocity distribution of the atomic beam was characterized in [26]. After preparation of atoms in the $2S_{1/2}^{F=0}$ state, the atoms enter the RF spectroscopy chamber. The RF spectroscopy region consists of two copper loops separated by a distance of 28 cm. Each loop is driven by an RF source to generate an oscillating magnetic field at ≈177 MHz to drive population from the $2S_{1/2}^{F=0}(m_F{=}0)$ state to the $2S_{1/2}^{F=1}(m_F{=}0)$ state. The RF sources use direct-digital-synthesis (DDS), and are referenced through an optical fiber link to a small ensemble of cesium beam clocks at the NIST WWV Radio Station, which is in turn referenced to UTC(NIST). Any remaining population in the $2S_{1/2}^{F=0}$ state is selectively quenched to the $2P_{1/2}^{F=1}$state using an oscillating electric field at ≈910 MHz produced by a parallel-plate capacitor. Atoms in the $2S_{1/2}^{F=1}$ state are then detected using a channel-electron multiplier

(CEM) in pulse-counting mode to give the final spectroscopic signal. The spectroscopy region is housed within a magnetic shield with a solenoid to produce a small bias magnetic field. Additionally, on both sides of each copper loop is an aluminum ring. These sets of aluminum rings serve to mitigate any net magnetic flux through the solenoid. Without these rings, the combination of RF loops and the solenoid resembles a transformer which could produce an unwanted RF voltage along the length of the solenoid. The entire RF spectroscopy region is coated in colloidal graphite to reduce stray DC electric fields. A schematic of the RF spectroscopy system is shown in Fig. 1.

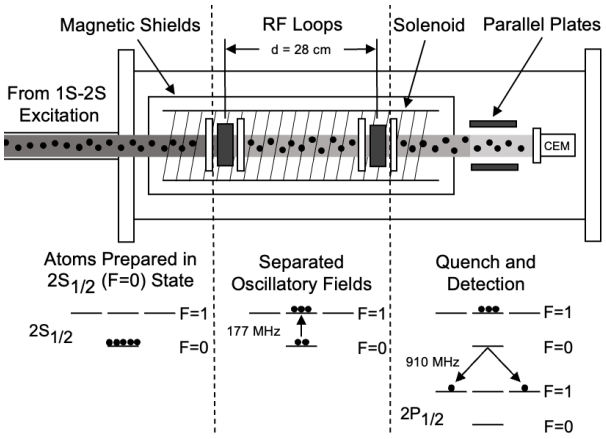

FIG. 1. Schematic of the experimental apparatus. Atoms initially prepared in the $2S_{1/2}^{F=0}$ state enter a magnetically shielded region where Ramsey spectroscopy is performed. A solenoid allows for a bias magnetic field to be applied. Any remaining population in the $2S_{1/2}^{F=0}$ state is selectively quenched to the $2P_{1/2}^{F=1}$state using an electric-dipole transition. The excited state population is detected using a CEM.

In Fig. 2, we show a typical Ramsey fringe obtained from our spectrometer. We have overlaid experimental data with a simulation obtained by integrating the Bloch equations given the time-dependent magnetic fields seen by the atoms as they traverse the spectrometer. For the simulation, we used the metastable atom velocity distribution measured previously in our apparatus [26]. As can be seen from the figure, the agreement with our simulation is excellent, which we believe is a testament to the relatively straightforward experimental apparatus.

A total of 17 measurement runs were performed over the course of two months in 2022. We usually obtained one measurement run in a given day where each run consisted of ≈ 300 individual scans of the resonance. Measurement runs were conducted at varied times of day and typically required six hours of cumulative data collection. Each scan of the resonance includes 32 frequencies about the central feature of the Ramsey fringe. For each scan, frequency points were taken in a new random order to eliminate potential systematic effects related to drifting atomic beam

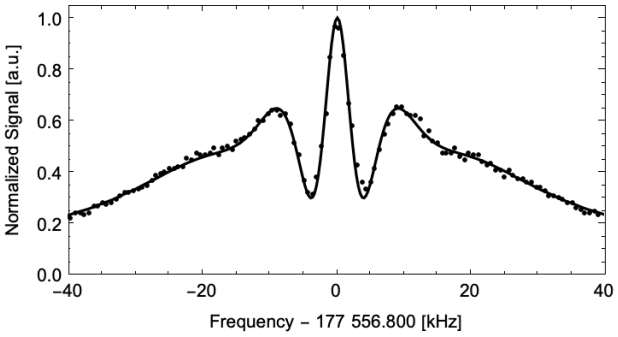

FIG. 2. Example lineshape from an average of 6 scans of the $2S_{1/2}^{F=0}(m_F=0)$ - $2S_{1/2}^{F=1}(m_F=0)$ resonance obtained using Ramsey spectroscopy with room temperature hydrogen beam with a numerical simulation overlaid. The FWHM of the central peak is approximately 4 kHz.

flux. The resonance was fit with a function, F, defined by

$$F = B + A\,\mathrm{sinc}^2\left(\frac{f - f_0}{\Gamma}\right), \tag{2}$$

where A and f_0 represent the amplitude and linecenter frequency, respectively, and Γ is proportional to the width of the lineshape. The offset, B, was included in the fit function because the Ramsey fringe minimum is not zero, in contrast to a sinc^2 function. While the use of a sinc^2 function is an approximation to the true central feature of the Ramsey fringe, we prefer to fit our data with simple analytic functions since it eliminates possible errors stemming from an incorrect numerical model, which necessarily has some assumptions. We also performed our data analysis using a Gaussian fit function and found that it altered our final result by only 0.08 Hz, which shows that our analysis was not, within reason, sensitive to the specific fit function.

A typical challenge to Ramsey spectroscopy is to ensure that there is no phase difference between the two RF spectroscopy regions. The frequency shift due to a phase difference, $\Delta\phi$, is inversely proportional to the time atoms spend between the two loops and is approximately

$$f_{\Delta\phi} = \frac{v\Delta\phi}{2\pi d}, \tag{3}$$

where v and d are the velocity of the atoms and distance between the RF loops, respectively. Since this systematic shift is proportional to the beam velocity, it can be considered a residual first-order Doppler shift. A common but challenging method to characterize and eliminate $\Delta\phi$ is to exchange the order of the two RF regions in the beamline as in [27]. However, since we have the ability to adjust the velocity of the hydrogen beam, we can perform a linear extrapolation of the measured linecenter as a function of velocity to extract the true linecenter. Thus, we do not need to eliminate $\Delta\phi$, but only require that it is stable during

a given measurement run.

During a measurement run, we randomly alternate between measurements with the atomic beam nozzle at 6 K and 30 K leaving all other experimentally-controlled parameters identical. To eliminate any long-term drifts in the phase between the RF loops, scans are binned, where a single bin includes 20-25 scans of the resonance at a given temperature. Additionally, the relative phase between the two RF loops is monitored using a setup similar to that in [27]. Directional couplers and RF mixers produce voltages proportional to the phase difference between the two incident and reflected signals, which are continuously monitored. We observe no significant drift in either phase over the course of any data collection day. Although the temperature of the cryogenic nozzle is constantly monitored, deviations between the temperature reading of the nozzle and the actual temperature of the hydrogen beam are possible, therefore we perform extrapolations of the linecenter as a function of the measured transit-time broadened linewidth for each bin, which is proportional to the beam velocity. The RF loop voltage was varied before every run to ensure that power broadening was negligible, and mean velocities determined from the obtained linewidths were consistent with the measured nozzle temperature.

An example extrapolation and the extracted linecenters from 17 data runs are shown in Fig. 3. While it may seem intuitive that such extrapolations are linear, the situation is somewhat more complicated since we measure a thermal velocity distribution and not a single velocity class. By simulating our lineshapes using thermal velocity distributions, we find that the extrapolations have a small error, which is proportional to $\Delta\phi$, with a maximum magnitude of 0.2 Hz. As an experimental check, we changed $\Delta\phi$ using DDS control for different measurement runs and observed no discrepancies in the extrapolated value. We include a 0.2 Hz uncertainty to account for this slight nonlinearity in the extrapolation.

The shift to the splitting of the $2S_{1/2}^{F=0}(m_F{=}0)$ - $2S_{1/2}^{F=1}(m_F{=}0)$ transition in the presence of a static magnetic field is quadratic and has the value 22.184 kHz/G^2 [20]. In order to characterize any residual field along the direction of the atomic beam remaining after magnetic shielding, we applied a bias field at various field strengths and measured the linecenter as shown in Fig. 4. We find a residual field of 0.14(13) mG, which agrees well with the simulated performance of our magnetic shield along with measurements of Earth's field near the apparatus.

The maximum magnetic field applied during the measurement runs shown in Fig. 3b is 24 mG. Taking into account the residual field and its uncertainty, we apply a correction of -13.26(28) Hz for data runs taken at this bias magnetic field. The uncertainty in the bias field correction is smaller for data runs taken at 8 and 16 mG magnetic fields; however, we conservatively add an uncertainty of 0.28 Hz to the total measurement due to the presence of residual magnetic fields.

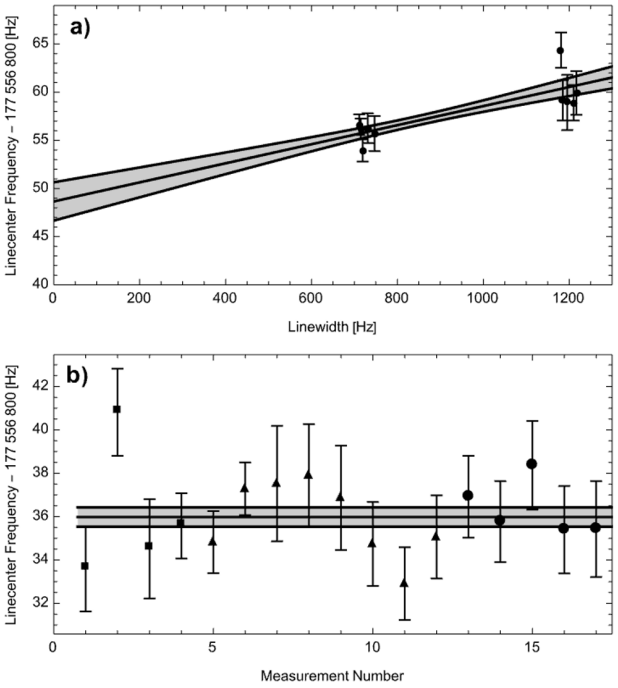

FIG. 3. a) Example phase shift extrapolation between temperatures of 6K and 30K as a function of the extracted linewidth. The shaded grey region corresponds to the one-standard-deviation confidence interval. b) Extrapolated zero-phase linecenters after bias magnetic field correction. Squares, triangles, and circles represent data taken at 8, 16, and 24 mG applied magnetic field, respectively. The shaded grey region represents one standard-deviation from the statistical mean. The reduced χ^2 for the 17 data-sets is 1.05.

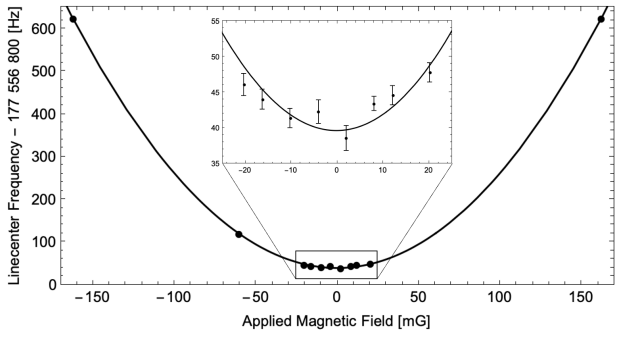

FIG. 4. Relative shift of the resonance as a function of applied magnetic field from solenoid. In the main figure, error bars are not included because they are too small to be visible.

While transition rates to the $2S_{1/2}^{F=1}(m_F{=}\pm\ 1)$ states should be small due to the polarization of the magnetic fields produced by the RF loops, the splitting of those states is a substantial $\pm$1.4 MHz/G. How-

ever, a shift in the measured resonance will only occur if the $2S_{1/2}^{F=1}(m_F=\pm\ 1)$ states are excited unequally, which would require some degree of circular RF polarization. Such circular polarization is unlikely given the RF loop design. Nevertheless, to quantify this effect, we measured the transition with the atomic beam at room temperature and with a bias field of ±1.5 mG. This places any spurious resonance directly on the side of the main peak. Upon reversal of the field, we observed no shift in the resonance up to our measurement precision of 4 Hz for this test. With this we are able to limit the relative imbalance of transitions to the $2S_{1/2}^{F=1}(m_F=\pm\ 1)$ states to 0.003 that of the main resonance. With the magnetic fields and beam temperatures used in the data shown in Fig. 3b, the $2S_{1/2}^{F=1}(m_F=\pm\ 1)$ transitions are far off-resonance and would pull the line by a maximum of 10^{-5} Hz.

As atoms traverse the regions near each of the RF loops, a small electric field is expected to be present due to the oscillating current at 177 MHz in the copper loops. This can produce an RF Stark shift through coupling of the $2S_{1/2}$ state to the $2P_{1/2}$ and $2P_{3/2}$ states. Since the shift in the linecenter as a function of the RF drive power is linear, we performed an extrapolation of the extracted linecenter as a function of the RF drive power to characterize this effect. For this test, the RF drive power was varied by a factor of sixteen, which was the maximum variation possible to produce sufficient signal-to-noise ratios while ensuring that saturation effects were negligible. We find that the shift due to the RF Stark effect is -2.85(63) Hz. This shift is reasonable given the residual level of electric field expected within the RF loops. There is also the possibility of an RF Stark shift from leakage of the 910 MHz field used to quench the $2S_{1/2}^{F=0}$ population. This field is well shielded from the interaction region and we measured > 55 db of attenuation outside of the quench region, which we estimate produces a < 0.007 Hz shift to the measurement.

The DC Stark shift is quadratic and has the value $\Delta f_{\rm DC} = -(880E^2 + 230E_z^2)$ Hz $(\rm cm/V)^2$ [20]. In order to mitigate this effect, the entire RF system was enclosed in a Faraday cage and coated with colloidal graphite. Previously, we have characterized the strength of DC electric fields using the same method to prepare the Faraday cage and found fields to be $\leq$6.5 mV/cm [25]. Therefore, we assume a stray field of 6.5 mV/cm in the radial direction and apply a shift of 0.037(37) Hz.

The collisional shift of the $2S_{1/2}$ hyperfine interval is on the order of 10 Hz/mBar [23]. All of the data collection was taken with background hydrogen pressure on the order of 10^{-8} mBar or lower, which we estimate is the dominant source of collisions. This leads to a negligible shift.

From the phase-extrapolated data after the bias magnetic field corrections we obtain a value for the $2S_{1/2}$ hyperfine interval of $f(2S_{1/2}) =$ 177 556 835.98(45) Hz. After correction due to other systematic effects, the value is $f(2S_{1/2}) =$ 177 556 838.87(85) Hz. All systematic corrections are summarized in Table I. Combining the measured value of the $2S_{1/2}$ hyperfine interval from this work and the experimentally determined value of the $1S_{1/2}$ hyperfine interval gives

$$D_{21} = 48\,959.2(6.8)\ \text{Hz}, \tag{4}$$

which is in good agreement with the theoretical value as shown in Fig. 5.

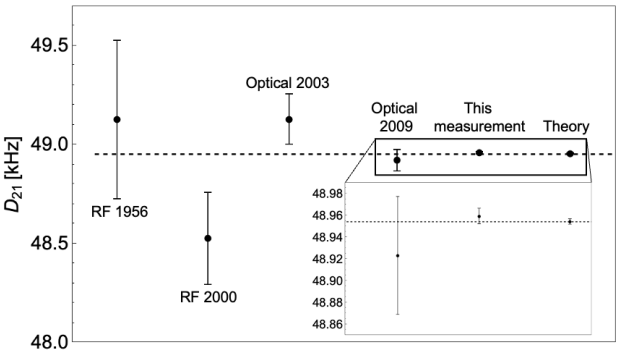

FIG. 5. Experimental (RF 1956 [20], RF 2000 [21], Optical 2003 [22], and Optical 2009 [23]) and theoretical [9] values of D_{21}. The dashed line represents the theoretical value.

TABLE I. Systematic corrections to the phase-extrapolated and magnetic field corrected $2S_{1/2}$ hyperfine interval.

	$f(2S_{1/2})$ [Hz]	σ [Hz]
Phase and bias field corrected	177 556 835.98	0.45
RF Stark effect (177 MHz)	2.85	0.63
RF Stark effect (910 MHz)	0	0.007
Residual magnetic fields	0	0.28
Extrapolation nonlinearity	0	0.2
DC Stark effect	0.037	0.037
Spurious transitions	0	10^{-5}
Collisional shift	0	10^{-7}
Second-order Doppler shift	0.001	0.001
Final measured value	177 556 838.87	0.85

Experimental values of D_{21} are also available for deuterium [28, 29] and the $^3He^+$ ion [30, 31]. Previously, constraints on light psuedo-vector bosons were similar in all three species [17]. However, with the results presented here, the constraints from hydrogen have been significantly improved. Therefore, we believe a new measurement of D_{21} in deuterium using RF Ramsey spectroscopy is well-motivated. While the theory value is currently 2.8 times more precise than our experimental measurement, further improvements could likely be achieved by increasing the distance between the RF loops in our Ramsey spectrom-

eter. With this, an investigation into the remaining sources of theoretical uncertainty in the fourth-order QED corrections may be warranted [6, 7].

In conclusion, we present a new measurement of the hydrogen $2S_{1/2}$ hyperfine interval. We have reduced the experimental uncertainty of this interval by a factor of ≈ 8 and find a value in good agreement with theory [6, 8], which provides a stringent test of bound-state QED. We note that added confidence in the bound-state QED corrections may be relevant for upcoming measurements of the ground state hyperfine splitting in muonic hydrogen, which aim to obtain precise information about the magnetic structure of the proton [32].

We gratefully acknowledge funding through a Center for Fundamental Physics grant from the John Templeton Foundation and Northwestern University, NSF Career Award #1654425, and NSF Award #2207298. We would like to thank Glenn Nelson, Matt Deutch, Bill Yates, Jim Spicer, Michael Lombardi, Judah Levine, and Jeffrey Sherman at NIST for assistance with the system of cesium beam clocks used for frequency calibration. Finally, we gratefully acknowledge Jacob Roberts, Sam Brewer, Savely Karshenboim, Ulrich Jentschura, Aldo Antognini, and Thomas Udem for useful discussions and comments on the manuscript.

[1] E. Tiesinga, P. J. Mohr, D. B. Newell, and B. N. Taylor, CODATA recommended values of the fundamental physical constants: 2018, Rev. Mod. Phys. **93**, 025010 (2021).

[2] Hellwig, H., R. F. Vessot, M. Levine, P. W. Zitzewitz, D. W. Allan, and D. T. Glaze, Measurement of the Unperturbed Hydrogen Hyperfine Transition Frequency, IEEE Trans. Instrum. Meas. **19**, 200 (1970).

[3] L. Essen, M. J. Donaldson, M. J. Bangham, and E. G. Hope, Frequency of the hydrogen maser, Nature **229**, 110 (1971).

[4] L. Essen, R. W. Donaldson, E. G. Hope, and M. J. Bangham, Hydrogen Maser Work at the National Physical Laboratory, Metrologia **9**, 128 (1973).

[5] P. Petit, M. Desaintfuscien, and C. Audoin, Temperature Dependence of the Hydrogen Maser Wall Shift in the Temperature Range 295-395 K, Metrologia **16**, 7 (1980).

[6] S. G. Karshenboim and V. G. Ivanov, Hyperfine structure of the ground and first excited states in light hydrogen-like atoms and high-precision tests of QED, Eur. Phys. J. D **19**, 13 (2002).

[7] S. G. Karshenboim and V. G. Ivanov, Hyperfine structure in hydrogen and helium ion, Phys. Letters B **524**, 259 (2002).

[8] U. D. Jentschura and V. A. Yerokhin, Quantum electrodynamic corrections to the hyperfine structure of excited S states, Phys. Rev. A. **73**, 062503 (2006).

[9] V. A. Yerokhin and U. D. Jentschura, Electron Self-Energy in the Presence of a Magnetic Field: Hyperfine Splitting g Factor, Phys. Rev. Lett. **100**, 163001 (2008).

[10] V. A. Yerokhin, A. N. Artemyev, V. M. Shabaev, and G. Pluien, All-order results for the one-loop QED correction to the hyperfine structure in light H-like atoms, Phys. Rev. A. **72**, 052510 (2005).

[11] M. I. Eides, H. Grotch, and V. A. Shelyuto, Theory of Light Hydrogenlike Atoms, Phys. Rep. **342**, 63 (2001).

[12] D. E. Zwanziger, α^3 Corrections to Hyperfine Structure in Hydrogenic Atoms, Phys. Rev. **121**, 1128 (1961).

[13] M. M. Sternheim, State-Dependent Mass Corrections to Hyperfine Structure in Hydrogenic Atoms, Phys. Rev. **130**, 211 (1963).

[14] S. G. Karshenboim, F. S. Pavone, G. F. Bassani, M. Inguscio, and T. W. Hänsch, *The Hydrogen Atom: Precision Physics of Simple Atomic Systems*, (Springer, Berlin, Heidelberg, 2001).

[15] S. G. Karshenboim, P. Fendel, V. G. Ivanov, N. N. Kolachevsky, and T. W. Hänsch, The 2s hyperfine structure in hydrogen and deuterium: a precision test of bound state quantum electrodynamics, Can. J. Phys. **83**, 283 (2005)

[16] S. G. Karshenboim, Precision physics of simple atoms: QED tests, nuclear structure and fundamental constants, Phys. Reports **422**, 1 (2005).

[17] S. G. Karshenboim, Precision Physics of Simple Atoms and Constraints on a Light Boson with Ultraweak Coupling, Phys. Rev. Lett. **104**, 220406 (2010).

[18] C. Frugiuele, C. Peset, Muonic vs electronic dark forces: a complete EFT treatment for atomic spectroscopy, JHEP **05**, 002 (2022)

[19] P. Fadeev, F. Ficek, M. G. Kozlov, D. Budker, and V. V. Flambaum, Pseudovector and pseudoscalar spin-dependent interactions in atoms, Phys. Rev. A **105**, 022812 (2022).

[20] J. W. Heberle, H. A. Reich, and P. Kusch, Hyperfine Structure of the Metastable Hydrogen Atom, Phys. Rev. **101**, 612 (1956).

[21] N. E. Rothery and E. A. Hessels, Measurement of the 2S atomic hydrogen hyperfine interval, Phys. Rev. A. **61**, 044501 (2000).

[22] N. Kolachevsky, M. Fischer, S. G. Karshenboim, and T. W. Hänsch, High-Precision Optical Measurement of the 2S Hyperfine Interval in Atomic Hydrogen, Phys. Rev. Lett. **92**, 033003 (2004).

[23] N. Kolachevsky, A. Matveev, J. Alnis, C. G. Parthey, S. G. Karshenboim, and T. W. Hänsch, Measurement of the 2S Hyperfine Interval in Atomic Hydrogen, Phys Rev. Lett. **102**, 213002 (2009).

[24] A. Beyer, *et al.*, The Rydberg constant and proton size from atomic hydrogen, Science **358**, 79 (2017).

[25] A. D. Brandt, S. F. Cooper, C. Rasor, A. Matveev, and D. C. Yost, Measurement of the $2S_{1/2} - 8D_{5/2}$ transition in hydrogen, Phys. Rev. Lett. **128**, 023001 (2022).

[26] S. F. Cooper, A. D. Brandt, C. Rasor, Z. Burkley, and D. C. Yost , Cryogenic atomic hydrogen beam apparatus with velocity characterization, Review of Scientific Instruments **91**, 013201 (2020)

[27] N. Bezginov, T. Valdez, M. Horbatsch, A. Marsman, A. C. Vutha, and E. A. Hessels, A measurement of the

atomic hydrogen Lamb shift and the proton charge radius, Science **365**, 1007 (2019).
[28] N. Kolachevsky, P. Fendel, S. G. Karshenboim, and T. W. Hänsch, 2S hyperfine structure of atomic deuterium, Phys. Rev. A **70**, 062503 (2004).
[29] D. J. Wineland and N. F. Ramsey, Atomic Deuterium Maser, Phys. Rev. A **5**, 821 (1972).
[30] H. A. Schuessler, E. N. Fortson, and H. G. Dehmelt, Hyperfine Structure of the Ground State of $^3He^+$ by the Ion-Storage Exchange-Collision Technique, Phys. Rev. **187**, 5 (1969).
[31] M. H. Prior and E. C. Wang, Hyperfine structure of the 2S state of $^3He^+$, Phys. Rev. A **16**, 6 (1977).
[32] A. Antognini, F. Hagelstein, V. Pascalutsa, "The proton structure in and out of muonic hydrogen", Annu. Rev. Nucl. Part. Sci. **72**, 389 (2022).